Available online at www.sciencedirect.com
ScienceDirect

Catalysis Today 117 (2006) 180–186

CATALYSIS TODAY

www.elsevier.com/locate/cattod

Selective oxidative activation of isobutane on a novel vanadium-substituted bimodal mesoporous oxide V-UVM-7

L.J. Huerta [a], P. Amorós [a], D. Beltrán-Porter [a], V. Cortés Corberán [b,*]

[a] *Institut de Ciència dels Materials (ICMUV), University of Valencia, P.O. Box 22085, 46071 Valencia, Spain*
[b] *Institute of Catalysis and Petroleumchemistry (ICP), CSIC, Marie Curie 2, 28049 Madrid, Spain*

Abstract

New vanado-silicates with a bimodal mesoporous system (V-UVM-7) and high vanadium contents ($Si/V \geq 7$) have been prepared by a modification of the so-called atrane method. Its morphology consists of aggregation of nano-particles with V-MCM-41 structure, creating a second broader porous system in their interparticle space. Its structure allows to incorporate a high V contents into tetrahedral sites of the framework while keeping vanadium dispersion. V-UVM-7 catalysts are very active and selective for the direct transformation of isobutane to isobutene and methacrolein. Total conversion and methacrolein-to-isobutene ratio in the products increased with increasing vanadium contents. The catalytic performance comparison with homologous V-MCM-41 catalysts revealed an influence of the channel length on the products distribution.

Keywords: Alkane selective oxidation; Methacrolein from isobutane; Nanosized V-MCM-41; UVM-7; Isobutane oxydehydrogenation

1. Introduction

The selective oxidative activation of light alkanes into olefins and unsaturated oxygenated products is a very attractive way for the valorization of large natural gas resources. However, oxidative dehydrogenation (ODH) of light alkanes, and that of isobutane in particular, is still an unresolved challenge. This is due to the higher reactivity for combustion of the products of interest compared to that of the starting alkane. As a consequence, the values of olefin selectivity, yield and productivity per unit mass of catalyst reached to date need to be significantly improved for this route to become economically feasible.

In principle, this could be done by maximizing the number of selective active centers per unit mass of catalyst. Most of the catalysts used for ODH of light alkanes are based on vanadium-containing oxides, whose properties depend strongly on the nature of V species (oxidation state, coordination sphere, dispersion, and stability) [1,2]. Supported vanadium oxide catalysts are more selective than the bulk V_2O_5, where vanadium atoms are in octahedral coordination [1]. Isolated or polymeric tetrahedral V^{5+} species, obtained by spreading the oxide onto a support [3–5] are the most selective for the oxidative dehydrogenation (ODH) to alkenes [1,3,6]. It has been reported that isolated tetrahedral vanadium species show the highest intrinsic activity for ODH [7,8], although there are still some discrepancies about the vanadium active species for the selective oxidation of alkanes [1,2]. Therefore, one way to improve the catalyst would be to synthesize it with the maximum vanadium dispersion, to get isolated centers, while keeping a high number of active centers. This can be done by dispersing vanadium into mesoporous oxides, such as MCM-41 silicas. The use of V-MCM-41 for ODH of ethane [9], propane [9–11] and isobutane [9,12,13] with oxygen has been recently reported.

A large variety of methods to incorporate V species in MCM-41-like silicas are described in literature, including ion-exchange [9], grafting [11], one-pot co-hydrolysis [9,11,14–17], impregnation [18,19] and chemical vapor deposition [20]. Regardless the synthesis strategy used, three main troubles usually occur with mesoporous V-containing silica catalysts: (1) the relatively low vanadium amount commonly achieved (<1 wt.%) [9] maintaining a good heteroelement dispersion, (2) the deleterious effect on the catalytic efficiency of the possible segregation of V_2O_5 microcrystals if vanadium exceeds that contents, and (3) the mass transport to and from the active sites located in the

---

* Corresponding author.
E-mail address: vcortes@icp.csic.es (V.C. Corberán).

0920-5861/$ – see front matter © 2006 Elsevier B.V. All rights reserved.
doi:10.1016/j.cattod.2006.05.016

internal mesopore walls through the straight, unconnected mesopores, what often results in pore blocking [21]. Independently or combined, these drawbacks can be considered as the responsible factors leading to undesired oxidative degradation products and low catalytic productivity.

The two first problems, dealing with the adequate incorporation of vanadium in the silica framework, can be solved by using the so-called atrane route, a simple one-pot strategy based on the use of atrane complexes (containing triethanolamine as ligand) as precursors [22]. We recently reported the preparation, through this atrane route, of V-MCM-41 catalysts with high vanadium content ($Si/V \geq 49$) having good heteroelement dispersion, and its use for the selective oxidation of isobutane [13]. These catalysts are very active and, besides the formation of isobutene, they catalyze the direct oxidation of isobutane to methacrolein with 30% selectivity, which allows to obtain the highest yields per pass for the direct oxidation of isobutane reported in literature. Interestingly, at similar isobutane conversions, the higher the V content in the V-MCM-41 material, the higher the conversion and the methacrolein selectivity and the lower the isobutene selectivity. However, an increase of V contents, i.e., for $Si/V < 49$, caused a loss of the hexagonal order and surface area, and an alternative is needed to further increase the vanadium contents along this approach.

Concerning the third limitation, a variety of alternative approaches have been classically adopted, such as the pore size expansion (SBA-15 like solids) and the use of interconnected mesoporous systems (MCM-48 like solids). Recently, an alternative strategy that is attracting much attention is focused on the synthesis of hierarchical multimodal porous materials [23]. These solids combine an enhanced accessibility to the active sites with high surface area and pore volume. Probably, the simplest strategy to obtain bimodal porous silicas is conceptually based on the consequences of decreasing the particle size of the mesoporous material to the nanoparticle range. This necessarily would imply, in principle, the shortening of the mesopore channel length, whereas the particle packing would generate supplementary inter-particle porosity [24]. In practice, the synthesis of nanoparticulated aluminum containing bimodal porous silicas was first described by Pauly et al. [25] who prepared the so-called Al-HMS materials. Later, our group reported the one-pot synthesis of nanoparticulated bimodal silicas of the UVM-7 family including variable amounts of heteroelements (Ti, Al, V, Zr) in the low and medium concentration range ($\infty \geq Si/M \geq 50$) [24]. We have adopted this synthesis strategy in order to increase the vanadium contents in the mesoporous catalysts without loosing the vanadium active center environment, and to improve the accessibility to the inner pore walls active centers, which should improve their intrinsic activity.

We report here for the first time the synthesis, characterization and catalytic behavior of a novel bimodal vanadium-containing mesoporous silica-based mixed oxide, denoted as V-UVM-7, whose structure allows to incorporate a higher V contents (up to $Si/V = 14$) than V-MCM-41, while keeping vanadium dispersion and mesopores regularity. Their catalytic properties for the selective oxidation of isobutane are explored and compared with those of V-MCM-41, which allows to analyze the influence of the particle size (and hence, of mesopore length) in the catalytic performance.

2. Experimental

2.1. Catalysts preparation

All the synthesis reagents (tetraethyl ortosilicate (TEOS), triethanolamine ($N(CH_2–CH_2–OH)_3$, hereinafter TEAH3) and octadecyltrimethylammonium bromide (C_{18}TMABr) are analytically pure, and were used as received from Aldrich.

V-UVM-7 catalysts were prepared by a modified atrane route [22]. The general aspects of this one-pot surfactant assisted procedure for synthesizing nanoparticulate bimodal mesoporous silicas (NBS) were previously described in a short communication [24]. In a typical synthesis to obtain catalyst with $Si/V = 26$, a mixture of TEOS (10.3 mL; 0.048 mol), NH_4VO_3 (0.23 g; 0.002 mol) and TEAH3 (22.3 mL, 0.17 mol) was heated at 150 °C for 10 min to prepare atrane complexes in TEAH3 medium. The resulting solution, containing 0.048 mol of Si-atrane and 0.002 mol of V-atrane species, was cooled down to 90 °C, and 4.56 g C_{18}TMABr (0.0125 mol) were added. Then, 80 mL of water were slowly added with vigorous stirring at 80 °C. After a few minutes, a white suspension resulted that was aged at room temperature for 4 h. The resulting mesostructured solid was then separated by centrifugation, washed with water and ethanol, and air dried. To obtain the final catalyst, the as-synthesized solid was calcined at 500 °C for 4 h under a static air.

Table 1
Selected physicochemical properties of V-UVM-7 catalysts

(Si/V)		$d(1\,0\,0)$ (nm)	a_0[a] (nm)	BET area (m^2/g)	Pore size small pore[b] (nm)	Pore size large pore[b] (nm)	Pore volume small pore[b] (cm^3/g)	Pore volume large pore[b] (cm^3/g)	Wall thickness[c] (nm)
Gel	Solid[d]								
50	40	4.70	5.43	1008	3.40	30.0	0.70	1.10	2.03
30	26	4.65	5.37	1007	3.20	33.0	0.73	1.07	2.17
15	14	4.70	5.43	982	3.40	45.0	0.73	0.75	2.03
7	7	4.60	5.31	798	3.20	73.3	0.59	0.49	2.11
3	3	–	–	89	3.10	–	0.05	0.15	–

[a] Cell parameters calculated assuming a hexagonal cell ($a_0 = 2 \times d(1\,0\,0)/3.5$).
[b] Calculated from the adsorption branch of the isotherms and using the BJH model.
[c] Pore wall thickness defined as the difference between a_0 and BJH small (regular) mesopore size.
[d] Si/V molar ratio in the porous samples estimated from EPMA.

Table 1 summarizes the main synthesis variables and physical data of the prepared V-UVM-7 catalysts. In all cases, the reagents molar ratio in the starting solution was adjusted to $(2-x)$ Si:x V:7 TEAH3:0.52 C_{18}TMABr:180 H_2O, where $x = 0.04$ (Si/V = 50), 0.07 (Si/V = 30), 0.14 (Si/V = 15), 0.33 (Si/V = 7) and 1 (Si/V = 3)).

2.2. Catalysts characterization

All catalysts were analyzed for Si and V by electron probe microanalysis (EPMA) using a Philips SEM-515 instrument. Si/V molar ratio values were averaged from EPMA data corresponding to ca. 50 different particles. Low-angle (i.e., 1–10° (2θ)) X-ray powder diffraction (XRD) data were recorded on a Seifert 3000TT θ–θ diffractometer using Cu Kα radiation. Patterns were collected in steps of 0.02° (2θ) for 25 s/step. TEM images were obtained by means of a JEOL JEM-1010 instrument operating at 100 kV and equipped with a CCD camera. Adsorption–desorption isotherms of nitrogen were carried out in a Micromeritics ASAP 2010 instrument. Room-temperature diffuse reflectance spectra were recorded (200–800 nm) using a Shimazdu UV-Vis 2501PC spectrophotometer.

2.3. Catalytic tests

Catalyst samples (0.2 g) were tested for the ODH de isobutane in a tubular, fixed-bed continuous reactor at 325–490 °C using an iC_4H_{10}–O_2–He feed (molar ratio 27:13.5:59.5), with on-line GC analysis of reactants and products. Void volume of the reactor was filled with SiC bits. Preliminary tests showed the absence of homogeneous reactions in the absence of catalysts [26]. Conversion, selectivity and yields were calculated on a C-atom basis, and expressed as mol%. In all tests mass and carbon balances were within 100 ± 5%.

3. Results and discussion

3.1. Synthesis strategy

The co-hydrolysis approach to mixed oxides is burdened with problems related to the different reactivity of the inorganic precursors, which frequently leads to phase segregation [27]. Our synthesis strategy to obtain the V-UVM-7 catalysts has been designed to overcome the problems associated with the great reactivity differences that characterize the most usual Si and V species, as well as to favor the stabilization of a bimodal porous array. The first aspect is guaranteed by the "atrane route", where TEAH3 is used as a complexing agent able to keep the oxide-forming elements in homogeneous solution without undergoing phase segregation [22,24], even after water addition. The formation of a bimodal pore system is associated to the nanoparticulated morphology of V-UVM-7 materials, and consequently a quick nucleation process together with a highly suppressed particle growth is required. To achieve these conditions fast hydrolysis (to achieve supersaturation) and condensation (to provide charged oligomers able to interact with surfactant cations) processes, as well as low silica solubility, are required to form a large number of small size nuclei as precursors of the primary mesoporous nanoparticles. Therefore, the buffered pH around 9 provided by the TEAH3 seems to be the procedural key for obtaining the bimodal mesoporous system [24].

3.2. Catalysts characterization

EPMA data (Table 1) show that all the reported samples are chemically homogeneous at the spot area scale. Hence, the catalysts can be considered as monophasic products with a good dispersion of the heteroelement into the inorganic walls, and segregation of crystalline V_2O_5 can be practically discarded even for the samples with the highest V contents (although formation of V_2O_5-like amorphous nanodomains should progress as the V content does). This result is consistent with the absence of V_2O_5 peaks in the high-angle region of the XRD patterns. The Si/V molar ratio in the final solid is close to that present in the mother solution (Table 1), which suggests that there is no preferential incorporation of Si or V into the final catalyst. This result is due to the harmonization of the Si and V species hydrolysis processes thanks to the atrane precursors.

Excepting the catalyst with the highest vanadium content, all solids display low-angle XRD patterns with one strong peak and one broad signal of relatively low intensity (Fig. 1), that can be associated to the (1 0 0) and the overlapped (1 1 0) and (2 0 0) reflections of a MCM-41-like hexagonal cell [28], respectively. These patterns are characteristic of hexagonal disordered mesoporous materials, and they only inform us about the existence of the intra-nanoparticle ordered mesopore ('small' pores) system. Regardless the vanadium content, the position of the XRD signals and, consequently, the a_0 cell parameter are practically unchanged (see Table 1). The loss of

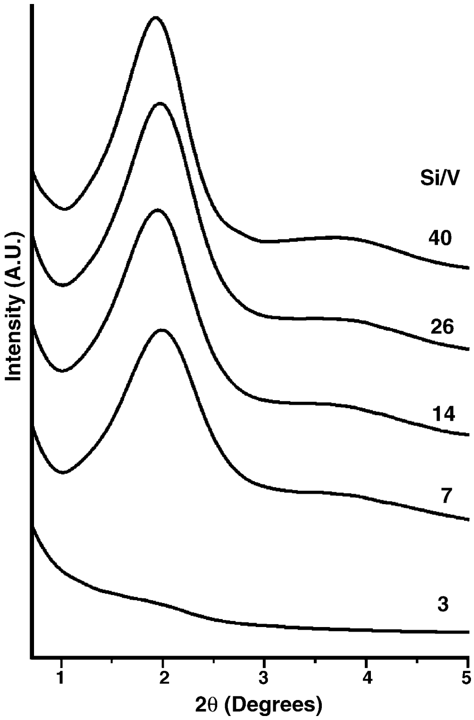

Fig. 1. Low-angle XRD patterns of V-UVM-7 catalysts.

peak intensity in the pattern of the solid with the highest V content must be attributed to a significant collapse of the mesostructure more than to loss of order, according to TEM and porosimetry data (see below).

TEM images (Fig. 2) show that the nanoparticulated bimodal porous structure typical of UVM-7 silicas is maintained up to very high vanadium contents (Si/V = 7). V-UVM-7 ($40 \geq$ Si/V ≥ 7) materials present a continuous nanometric organization built from aggregates of small mesoporous nanoparticles (connected through covalent bonds) that generate a hierarchic non-ordered system of inter-particle pores ('large' pores). The shape of the nanoparticles evolves from regular elliptical to irregular as the vanadium content increases. Simultaneously, a slight size reduction is detected. This leads to more dense aggregates, and hence to a lower inter-particle porosity, as the V content increases. The particulate morphology is yet maintained for the richest vanadium sample (Si/V = 3), but the intra-particle mesopores disappear.

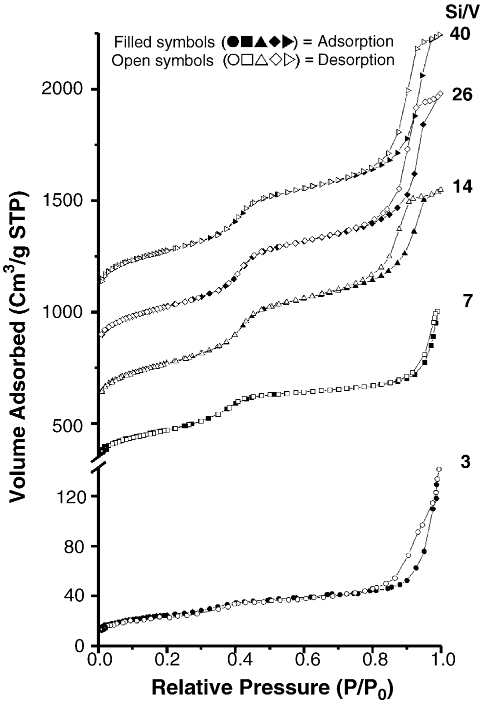

Fig. 3. N_2 adsorption-desorption isotherms of V-UVM-7 catalysts.

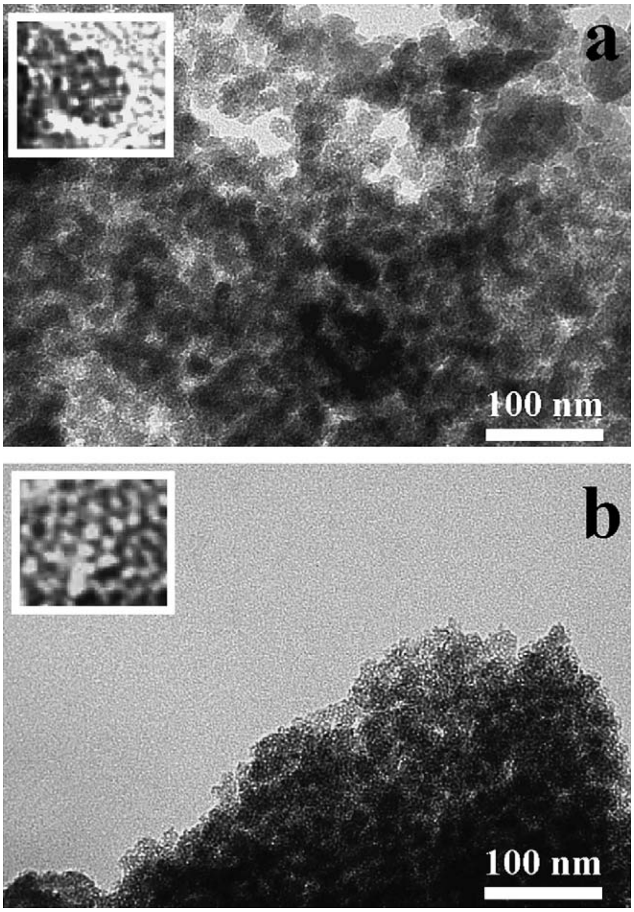

Fig. 2. Representative TEM images of V-UVM-7 catalysts: (a) Si/V = 40; (b) Si/V = 7. The intra-particle mesopore systems can be appreciated in the insets (enlarged (4×) images).

The bimodal pore system was further characterized by N_2 adsorption–desorption isotherms (Fig. 3). In the $40 \geq$ Si/V ≥ 7 compositional range all catalysts show curves typical of UVM-7 materials, with two well-defined steps. The first one, at intermediate partial pressures ($0.3 < P/P_0 < 0.5$) is due to the capillary condensation of N_2 inside the intra-nanoparticle mesopores. The second step, at a high relative pressure ($P/P_0 > 0.8$), corresponds to the filling of the large inter-particle cage-like pores. The pore size distributions (BJH) for the samples (Fig. 4) show clearly this bimodal character, with very homogeneous smaller intra-particle mesopores and more heterogeneous broader (>10 nm) inter-particle pores. These facts, and the high surface achieved, confirm that the UVM-7-like bimodal porous topology is maintained up to high vanadium loadings (Si/V = 7). In this compositional range the BET surface area smoothly decreases as the V content increases. The intra-particle mesoporous system remains practically unchanged with vanadium content. Thus, application of the BJH model leads to practically constant pore sizes (ca. 3.3 ± 0.1 nm) and pore volumes (0.6–0.73 cm^3/g) when varying the vanadium content. On the contrary, with regard to the inter-particle large pore system, the situation varies

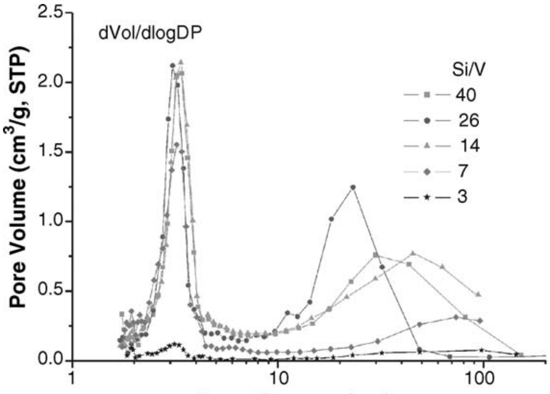

Fig. 4. BJH pore size distribution of the V-UVM-7 catalysts.

substantially, and it results clearly influenced by the Si/V ratio: the magnitude of the second adsorption effect in the isotherms gradually decreases (Fig. 3) and the broader pore system decreases (Fig. 4) as the V amount increases.

The pore wall thickness (estimated from XRD and porosity data) is larger than the observed for similar materials prepared from other reagents, and remains practically constant with the V content (Table 1). In fact, the stabilization of thick pore walls seems to be a common characteristic of all mesoporous solids isolated through the atrane method. This feature probably favors their comparatively high thermal stability.

Finally, although the isotherm of the vanadium richest sample (Si/V = 3) also displays two adsorption steps, the significant decrease of the respective pore volumes and the low BET area (compared to the other samples) clearly shows that a great collapse of the two pore systems occurs.

In conclusion, high vanadium content bimodal mesoporous catalysts have been synthesized in a wide compositional range (down to Si/V $\geq$ 7). Such a lower limit value corresponds to a V content significantly higher than those previously reported in the literature (maximum values around Si/V = 20) by using surfactants or block-copolymers as supramolecular templates [9,11,14–20].

Diffuse reflectance UV–vis spectroscopy was used to obtain additional information on the nature and environment of V species in V-UVM-7 catalysts. UV–vis spectra of V-UVM-7 samples recorded under ambient conditions (Fig. 5) shows the absence of adsorption bands in the 600–700 nm range (energy values typically associated to d–d electronic transitions) [29], allows to discard the existence of V(IV) centers. This fact is consistent with the yellow color of the samples. In all cases, the spectra display two intense and wide absorption bands at ca. 261 and 370 nm that have been assigned to charge–transfer transitions of V(V) sites in tetrahedral and penta- or hexa-coordinated environments, respectively [29–32]. The slight blue shift observed for the low energy band indicates that the vanadium centers are well dispersed. Then, isolated mono-nuclear V species are dominant, although the existence of a low proportion of oligomeric entities cannot be discarded. This fact is also supported by the quick and reversible color changes during successive dehydration (white)–rehydration (yellow) cycles, that are hindered in the case of oligomeric species. The band at ca. 261 nm is associated to V(V) species incorporated in the framework and inaccessible to water molecules, and the band at 370 nm can be attributed to V(V) sites close to the pore surface and, hence, highly accessible to water molecules. The similar intensity of both bands indicates that there is a similar proportion of internal and external V sites. This fact was not observed for V-MCM-41 materials prepared by the atrane method [13], for which the intensity of the band associated to internal tetrahedral V(V) species was significantly higher than the signal due to accessible sites. This different behavior supports the presence of a higher proportion of accessible catalytic centers in the V-UVM-7 catalysts as compared to V-MCM-41 catalysts.

Excepting the sample with the highest V amount (Si/V = 3), all calcined V-UVM-7 materials were white immediately after their calcination. Under this condition (just calcined, with no interaction with ambient atmosphere) the expansion of the vanadium coordination number does not occur. Moreover, taking into account the conditions of the isobutane ODH catalytic test, these anhydrous V centers must be the real catalytic sites. Thus, we have recorded the UV–vis spectra of selected samples (Fig. 6) before hydration and under dry conditions. After dehydration the adsorption band centered at ca. 370 nm, associated to the oxygen to vanadium charge–transfer transitions of square–pyramidal and/or octahedral V(V) chromophores [29–32], clearly disappears. Then, only one intense high energy complex band is observed in the spectra of the anhydrous catalysts. This band contains the signal due to the non-accessible tetrahedral vanadium sites inserted in the silica framework, and also the contribution of the new tetrahedral sites generated through dehydration. In fact, in the spectrum of the more diluted vanadium sample (Si/V = 40), we can observe, together with the intense adsorption at 252 nm, one shoulder at ca. 240 nm that can be attributed to distorted tetrahedral vanadium environments [29–32]. These sites corresponds to dehydrated penta- or octahedral vanadium original sites located at the silica surface. Moreover, another shoulder is observed at slightly low energy (ca. 300 nm). According to literature [29–32], this signal can be due to the presence of a small proportion of oligomeric tetrahedral V

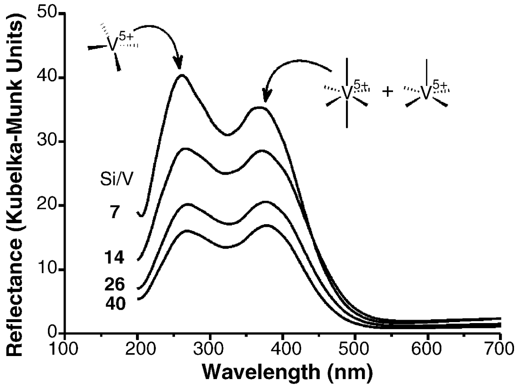

Fig. 5. Diffuse reflectance UV–vis spectra (recorded under ambient conditions) of V-UVM-7 catalysts.

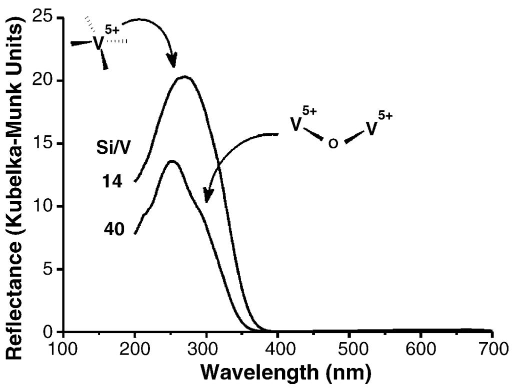

Fig. 6. Diffuse reflectance UV–vis spectra of selected V-UVM-7 anhydrous catalysts.

species, and probably also exists in the spectra of the hydrated samples. Broad UV–vis adsorption bands are recorded for the anhydrous samples as the vanadium content increases (Si/V = 14). This is probably due to the presence of a large variety of tetrahedral vanadium (isolated and oligomeric) sites with different distortion levels.

Summarizing, V-UVM-7 catalysts synthesized by the atrane method can be viewed as agglomerations of nanoparticles having a V-MCM-41 mesoporous structure with hexagonal symmetry and pore lengths (equivalent to the primary particles size) of the order of few nm. The chemical bonding between these agglomerated nanoparticles creates a second, broader and irregular, pore system. This architecture can accommodate a high amount of vanadium atoms ($Si/V \geq 7$) in tetrahedral coordination (in the anhydrous state), while keeping a high proportion of them accessible to reactants.

3.3. Catalytic activity

V-UVM-7 samples having an ordered mesoporous system, i.e. with $14 \leq Si/V \leq 40$, were tested as catalysts for the selective oxidation of isobutane. In the reaction conditions used, these catalysts were very active, the reaction products being detected already at 300 °C. As previously found on V-MCM-41 catalysts prepared by the atrane route [13], isobutene, methacrolein (MAL), acetone (ACT) and carbon oxides (COx) were the main products, accounting for near 90 mol% of the total. The formation of meaningful amounts of the selective oxidation product of isobutene (methacrolein) has also been observed on V-MCM-41 catalysts prepared via the atrane method [13], while has not been reported on similar catalysts prepared by other methods. Oxidative degradation and cracking products were also detected, especially at the higher temperatures. In all cases, start-up activity initially decreased down to a steady-state value, which was reached after 1 h on stream. Some representative steady-state catalytic data are shown in Table 2. Similar trends were observed with the three samples. The catalysts were very selective to ODH: taking into account that methacrolein is the product of the selective oxidation of isobutene, the overall dehydrogenation selectivity varies between 80 and 58% within the conversion range obtained (Table 2). Besides, selectivity to CO_x was very low, which is consistent with the absence of segregated V_2O_5 phase. Similar trends in selectivity evolution with conversion were observed for the three samples.

The catalytic performance depended strongly on the vanadium contents. The apparent activation energy (around 20–26 kcal/mol) decreased with increasing vanadium contents. Besides, when comparing at equal temperature, the isobutane conversion increased linearly with the V-contents (Table 2), with a slope bigger than unity. On the other hand, when comparing at equal conversion degree, the ratio methacrolein/isobutene increased with increasing V-contents. This selectivity ratio is indicative of the relative rates of isobutene oxidation to methacrolein and its formation from isobutane. Thus, these two findings could mean that, when the amount of V increased, the newly generated active centers were more active that the previous ones, and that they favor the oxidation of isobutene to methacrolein. The increase of isobutene oxidation to MAL (as shown by the increase of methacrolein/isobutene ratio) at isoconversion with the increase of vanadium content is parallel to the increasing concentration of low oligomeric V^{5+} species that could be expected with the increase of vanadium loading in the studied range [20,33]. These experimental results are consistent with the assumption, previously proposed to explain the formation of methacrolein on V-MCM-41 synthesized by the atrane route [13], that the isolated tetrahedral V^{5+} species is responsible to the ODH of isobutane to isobutene, and the low oligomeric V^{5+} species may be active for the formation of methacrolein.

3.4. Comparison with V-MCM-41: effect of mesopore channel length

These catalytic features, similar to those observed with V-MCM-41, could be expected because of their similar nature and structural features. Indeed, V-UVM-7 can be considered as a kind of nanosized V-MCM-41. In this structure the mesopores

Table 2
Selective oxidation of isobutane over V-UVM-7 catalysts[a]

Catalyst Si/V ratio	Reaction temperature (°C)	Conversion (%)		Selectivity (%)								Yield (%)	
		iC_4H_{10}	O_2	iC_4H_8	MAL[b]	ACT[c]	C_3H_6	HCHO	CO	CO_2	Others	iC_4H_8	MAL
40	400	1.3	1.7	59.4	21.1	4.1	0	0	6.3	9.2	0	0.79	0.28
	425	2.7	5.5	54.1	19.3	5.0	0	0	8.0	10.8	2.7	1.46	0.52
	450	5.4	18.0	46.9	17.6	4.9	6.4	0.3	9.7	11.7	2.5	2.53	0.95
	475	9.5	38.9	42.6	18.0	4.7	5.9	0.8	12.0	13.4	2.6	4.05	1.71
	490	12.5	54.5	41.0	17.3	4.3	4.9	1.1	13.8	14.5	3.0	5.11	2.16
26	400	3.3	12.4	48.9	21.4	5.2	0	0	8.5	12.6	3.0	1.58	0.69
	450	9.4	44.5	37.7	20.0	5.8	2.7	1.7	13.3	15.6	3.2	3.52	1.87
14	400	7.2	38.4	25.0	18.6	6.4	4.2	1.2	15.8	21.4	7.4	1.82	1.29
	410	8.9	45.0	22.4	15.9	5.7	5.0	7.0	14.8	20.6	8.4	2.02	1.41

[a] Feed: $iC_4:O_2:He = 27.0:13.5:59.5$ (mol%), W/F = 7.5 g_{cat} h/(mol_{C4}).

[b] MAL: methacrolein.

[c] ACT: acetone.

are unidirectional, parallel and not interconnected. Hence, the mesopore channel length is equal to the particle length along the *x*-axis, i.e., micrometric for V-MCM-41 and nanometric-sized for V-UVM-7. Therefore, by comparing the catalytic performance of these two types of materials with similar Si/V ratios, one may get information on the influence of channel length, and on the average residence time inside the channel, on the catalytic behavior.

By comparing the values in Table 1 for V-UVM-7 (Si/V = 40) at 475 °C, i.e., 9.5% conversion for W/F = 7.5 g_{cat} h/(mol_{C4}), with selectivity of 42.6% isobutene and 18.0% MAL, with those previously reported at equal temperature for V-MCM-41 (Si/V = 49), i.e., 10.6% conversion for W/F = 12 g_{cat} h/(mol_{C4}), with selectivity of 35.1% isobutene and 28.7% MAL [13], one may see that the activity per (total) V atom is around 20% higher for V-UVM-7, while the ratio methacrolein/isobutene is almost double in V-MCM-41, although their combined selectivity is similar. This implies that, besides the nature of the vanadium centers, the length of the mesopores also plays a role in determining the product distribution: the longer the channel, the higher the conversion (of isobutene) to methacrolein. This will support the recently proposed hypothesis of the contribution of heterogeneously initiated, radical gas-phase homogenous reactions inside the void volume of the mesopores of M-MCM-41 catalysts to its catalytic activity [34].

4. Conclusions

The atranes route allows to prepare a new type of bimodal mesoporous vanadosilicates with MCM-41-like structure without loss of the mesoporous hexagonal order for V contents up to Si/V $\geq$ 14. These V-UVM-7 materials constitute a new type of oxide catalysts active and very selective for ODH of isobutane and its oxidation to methacrolein, which structure can accommodate a very high content of vanadium (up to Si/V $\geq$ 7) in tetrahedral environments in the framework, mostly isolated but also low oligomeric. This allows an improved productivity in the selective oxidation of isobutane, with high selectivity to isobutene and methacrolein, which can be modulated by the vanadium contents. The comparison of their catalytic performance with that of homologous V-MCM-41 catalysts reveals that mesoporous channel length influences the product distribution, which could indicate a contribution of heterogeneously initiated, radical gas-phase homogenous reactions inside the void volume of the mesopores.

Acknowledgements

Funding by Spanish DGES (projects MAT2000-1387 and MAT2003-01696) and European Commission through the Coordination Action CONCORDE (NMP-CT-2004-505834) is gratefully acknowledged.

References

[1] E.A. Mamedov, V. Cortés Corberán, Appl. Catal. A: Gen. 127 (1995) 1.
[2] S. Albonetti, F. Cavani, F. Trifirò, Catal. Rev. Sci. Eng. 38 (1996) 413.
[3] G. Centi, F. Trifirò, J.R. Ebner, V. Franchetti, Chem. Rev. 88 (1988) 55.
[4] L. Owens, H.H. Kung, J. Catal. 144 (1993) 202.
[5] P. Concepción, J.M. López-Nieto, J. Pérez-Pariente, Catal. Lett. 19 (1993) 333.
[6] J. LeBars, J.C. Védrine, A. Auroux, S. Trautmann, M. Baerns, Appl. Catal. A 88 (1992) 179.
[7] R.X. Valenzuela, V. Cortés Corberán, Top. Catal. 11/12 (2000) 153.
[8] A. Pérez Pujol, R.X. Valenzuela, A. Fuerte, E. Wloch, A. Kubacka, Z. Olejniczak, B. Sulikowski, V. Cortés Corberán, Catal. Today 78 (2003) 247.
[9] Q. Zhang, Y. Wang, Y. Ohishi, T. Shishido, K. Takehira, J. Catal. 202 (2001) 308.
[10] J. Santamaría-González, J. Luque-Zambrana, J. Mérida-Robles, P. Maireles-Torres, E. Rodríguez-Castellón, A. Jimenez-López, Catal. Lett. 68 (2000) 67.
[11] M.L. Peña, A. Dejoz, V. Fornés, F. Rey, M.I. Vazquez, J.M. López Nieto, Appl. Catal. A 209 (2001) 155.
[12] B. Sulikowski, Z. Olejniczak, E. Wloch, J. Rakoczy, R.X. Valenzuela, V. Cortés Corberán, Appl. Catal. A 232 (2002) 189.
[13] M.J. Jia, R.X. Valenzuela, P. Amorós, D. Beltrán, J. El Haskouri, M.D. Marcos, V. Cortés Corberán, Catal. Today 91/92 (2004) 43.
[14] B. Solsona, T. Blasco, J.M.L. Nieto, M.L. Peña, F. Rey, A. Vidal-Moya, J. Catal. 203 (2001) 443.
[15] M. Mathieu, P. Van Der Voort, B.M. Weckhuysen, R.R. Rao, G. Catana, R.A. Schoonheydt, E.F. Vansant, J. Phys. Chem. B 105 (2001) 3393.
[16] Y. Yang, S. Lim, C. Wang, D. Harding, G. Haller, Microp. Mesop. Mater. 67 (2004) 245.
[17] S. Shylesh, A.P. Singh, J. Catal. 233 (2005) 359.
[18] N. Lang, P. Delichere, A. Tuel, Microp. Mesop. Mater. 56 (2002) 203.
[19] C. Hess, J.D. Hoefelmeyer, T. Don Tilley, J. Phys. Chem. B 108 (2004) 9703.
[20] G. Gruber, J. Rathouski, G. Schultz-Ekloff, M. Wark, A. Zukal, Microp. Mesop. Mater. 22 (1998) 225.
[21] D.R. Rolison, Science 299 (2003) 1698.
[22] S. Cabrera, J. El Haskouri, C. Guillem, J. Latorre, A. Beltrán, D. Beltrán, M.D. Marcos, P. Amorós, Solid State Sci. 2 (2000) 405.
[23] B. Zhang, S.A. Davis, S. Mann, Chem. Mater. 12 (2002) 1369, and references therein.
[24] J. El Haskouri, D. Ortiz de Zárate, C. Guillem, J. Latorre, M. Caldés, A. Beltrán, D. Beltrán, A.B. Descalzo, G. Rodriguez, R. Martínez-Mañez, M.D. Marcos, P. Amorós, Chem. Commun. (2002) 330.
[25] T.R. Pauly, Y. Liu, T.J. Pinnavaia, S.J.L. Billinge, T.P. Rieker, J. Am. Chem. Soc. 121 (1999) 8835.
[26] V. Cortés Corberán, M.J. Jia, J. El-Haskouri, R.X. Valenzuela, D. Beltrán-Porter, P. Amorós, Catal. Today 91/92 (2004) 127.
[27] G.J. de A.A. Soler-Illia, C. Sanchez, B. Lebeau, J. Patarin, Chem. Rev. 102 (2002) 4093, and references therein.
[28] C.T. Kresge, M.E. Leonowicz, W.J. Roth, J.C. Vartuli, J.S. Beck, Nature 359 (1992) 710.
[29] S. Dzwigaj, Curr. Opin. Solid State Mater. Sci. 7 (2003) 461.
[30] M.F. Hazenkamp, F.B. Van Duijneveldt, G. Blasse, J. Phys. Chem. 169 (1993) 55.
[31] J.S. Reddy, P. Liu, A. Sayari, Appl. Catal. A 148 (1996) 7.
[32] S. Dzwigaj, M. Matsuoka, M. Anpo, M. Che, J. Phys. Chem. B 104 (2000) 6012.
[33] M. Schraml-Marth, A. Wokaun, M. Pohl, H.L. Krauss, J. Chem. Soc., Faraday Trans. 87 (1991) 2635.
[34] V. Cortés Corberán, Catal. Today 99 (2005) 33.